



# CHORUS

This is the accepted manuscript made available via CHORUS. The article has been published as:

## Macroscopically Degenerate Exactly Solvable Point in the Spin-1/2 Kagome Quantum Antiferromagnet

Hitesh J. Changlani, Dmitrii Kochkov, Krishna Kumar, Bryan K. Clark, and Eduardo Fradkin

Phys. Rev. Lett. **120**, 117202 — Published 13 March 2018

DOI: [10.1103/PhysRevLett.120.117202](https://doi.org/10.1103/PhysRevLett.120.117202)

# The mother of all states of the kagome quantum antiferromagnet

Hitesh J. Changlani,<sup>1,2</sup> Dmitrii Kochkov,<sup>2</sup> Krishna Kumar,<sup>2</sup> Bryan K. Clark,<sup>2</sup> and Eduardo Fradkin<sup>2</sup>

<sup>1</sup>*Department of Physics and Astronomy, Johns Hopkins University, Baltimore, Maryland 21218, USA*

<sup>2</sup>*Department of Physics and Institute for Condensed Matter Theory,*

*University of Illinois at Urbana-Champaign, 1110 West Green St, Urbana IL 61801, USA*

(Dated: February 8, 2018)

Frustrated quantum magnets are a central theme in condensed matter physics due to the richness of their phase diagrams. They support a panoply of phases including various ordered states and topological phases. Yet, this problem has defied solution for a long time due to the lack of controlled approximations which make it difficult to distinguish between competing phases. Here we report the discovery of a special *quantum* macroscopically degenerate point in the  $XXZ$  model on the spin 1/2 kagome quantum antiferromagnet for the ratio of Ising to antiferromagnetic transverse coupling  $J_z/J = -1/2$ . This point is proximate to many competing phases explaining the source of the complexity of the phase diagram. We identify five phases near this point including both spin-liquid and broken-symmetry phases and give evidence that the kagome Heisenberg antiferromagnet is close to a transition between two phases.

The history of quantum frustrated magnetism began in 1973 with Anderson's suggestion that the ground state of the nearest-neighbor (n.n.) Heisenberg model on the triangular lattice was a quantum spin-liquid [1]. While we now know that this particular model does not support a spin-liquid, both experimental and theoretical evidence has been building for quantum spin-liquids in various lattices built of triangular motifs. Materials such as Herbertsmithite (a kagome lattice of  $\text{Cu}^{2+}$  ions) [2] and  $\text{Na}_4\text{Ir}_3\text{O}_8$  (a hyper-kagome lattice of  $\text{Ir}^{4+}$  ions) [3] fail to order down to low temperatures suggesting a possible spin-liquid ground state. This is supported by theoretical calculations which show that a panoply of spin-liquids (or exotic ordered phases) occur in a variety of Hamiltonians [4–17]. This Letter presents an explanation of multiple energetically competitive phases in these models.

We first report the existence of a new macroscopic *quantum* degenerate point on kagome and hyper-kagome lattices in the spin-1/2  $XXZ$  Hamiltonian [18–23],

$$H_{XXZ}[J_z] = \sum_{\langle i,j \rangle} S_i^x S_j^x + S_i^y S_j^y + J_z \sum_{\langle i,j \rangle} S_i^z S_j^z \quad (1)$$

at  $H_{XXZ}[-1/2]$  (notated as  $H_{XXZ0}$  [24]).  $S_i$  are spin-1/2 operators on site  $i$ ,  $\langle i, j \rangle$  refer to nearest neighbor pairs and  $J_z$  is the Ising coupling. The degeneracy exists in all  $S_z$  sectors and all finite system sizes. For kagome, we explicitly demonstrate this in Fig. 1 where we perform an exact diagonalization (ED) on the  $N = 30$  site kagome cluster in different  $S_z$  sectors. As we approach  $J_z = -1/2$  many eigenstates collapse to the same ground state eigenvalue.

We solve analytically for much of the exponential manifold, and our solutions apply to any lattice of triangular motifs with the Hamiltonian of the form,

$$H = \sum_{\Delta} H_{XXZ0}(\Delta) \quad (2)$$

where  $H_{XXZ0}(\Delta)$  is the  $XXZ0$  Hamiltonian on a triangle  $\Delta$ , as long as its vertices can be colored by three colors with no two connected vertices being assigned the same color. Some

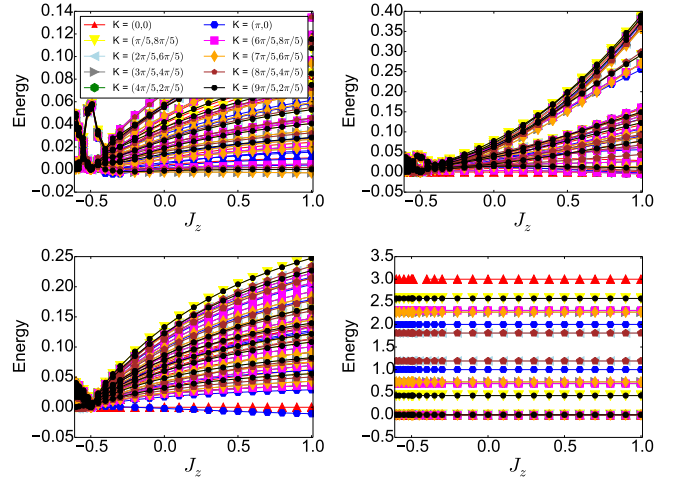


Figure 1. (Color online) Energy spectra (showing the 8 lowest energies in every momentum sector with respect to the lowest energy state in  $K = (0, 0)$ ) versus  $J_z$  for a 30 site kagome cluster with periodic boundary conditions. The panels correspond to various  $S_z$  sectors, (top left)  $S_z = 0$ , (top right)  $S_z = 5$ , (bottom left)  $S_z = 10$ , (bottom right)  $S_z = 14$ . A quantum degeneracy is seen at  $J_z = -1/2$ . The case of  $S_z = 14$  corresponds to one spin down in a sea of up spins and maps to the non-interacting solution, hence the spectrum does not change with  $J_z$ .

three-colorable lattices with representative three-colorings are shown in Fig. 2. Our general result overlaps the  $XXZ0$  point on the triangular lattice of Ref. [25] and a different analytically solvable Hamiltonian on the zig-zag ladder of Ref. [26].

Finally, we show how the  $XXZ0$  point on the kagome lattice is embedded in the wider phase diagram demonstrating its relation to the previously discovered spin-liquid at the Heisenberg point [7, 8, 10] as well as nearby magnetically ordered phases; our results suggest an additional intermediate phase transition in the middle of the spin-liquid region.

*Exact Ground States at  $J_z = -1/2$  — Any Hamiltonian of*

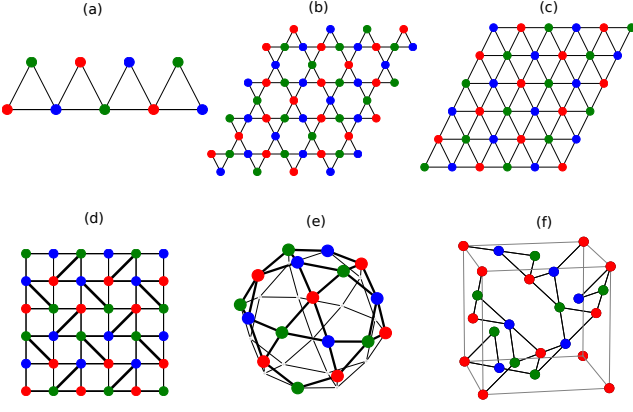


Figure 2. (Color online): Representative three-coloring solutions on various lattices with triangular motifs. (a) Saw-tooth (b) Kagome (c) Triangular (d) Shastry-Sutherland [27] (with  $J_2 = 2J_1$ , note, the bold diagonal lines are associated with two triangles whereas other edges are part of only one triangle) (e) Icosidodecahedron (f) Hyper-kagome lattice

the form of Eq. (2) has ground states of the form

$$|C\rangle \equiv P_{S_z} \left( \prod_{\text{valid}} \otimes |\gamma_s\rangle \right) \quad (3)$$

where  $\{|\gamma_s\rangle = |a\rangle, |b\rangle \text{ or } |c\rangle\}$ , denoted as "colors" on site  $s$  are defined as,  $|a\rangle \equiv \frac{1}{\sqrt{2}}(|\uparrow\rangle + |\downarrow\rangle)$ ,  $|b\rangle \equiv \frac{1}{\sqrt{2}}(|\uparrow\rangle + \omega|\downarrow\rangle)$ ,  $|c\rangle \equiv \frac{1}{\sqrt{2}}(|\uparrow\rangle + \omega^2|\downarrow\rangle)$ , where  $\omega = e^{i2\pi/3}$ . Taking the quantization axis to be the  $z$ -axis, the colors correspond to spin directions in the  $XY$  plane that are at 120 degrees relative to one another. Valid colorings satisfy the three-coloring condition.  $P_{S_z}$  projects into a particular total  $S_z$  sector.

For  $J_z = -1/2$  and a single triangle, six states; the fully polarized state  $|\uparrow\uparrow\uparrow\rangle$  and the chiral states  $|\uparrow\downarrow\downarrow\rangle + \omega|\downarrow\uparrow\downarrow\rangle + \omega^2|\downarrow\downarrow\uparrow\rangle$  and  $|\uparrow\downarrow\downarrow\rangle + \omega^2|\downarrow\uparrow\downarrow\rangle + \omega|\downarrow\downarrow\uparrow\rangle$  and all their Kramers pairs; are exactly degenerate. Thus Eq. (2) is recast as,

$$H = \sum_{\Delta} H_{\Delta} = \frac{3}{2} \sum_{\Delta} P_{\Delta} - \frac{3}{8} N_{\Delta} \quad (4)$$

where  $N_{\Delta}$  is the number of triangles and  $P_{\Delta}$  is a projector on the triangle  $P_{\Delta} \equiv |+\rangle\langle+| + |-\rangle\langle-|$  and  $|+\rangle$  and  $|-\rangle$  are Kramers pairs of non-chiral one-magnon states on the triangle,  $|+\rangle \equiv \frac{1}{\sqrt{3}}(|\uparrow\uparrow\downarrow\rangle + |\uparrow\downarrow\uparrow\rangle + |\downarrow\uparrow\uparrow\rangle)$  and  $|-\rangle \equiv \frac{1}{\sqrt{3}}(|\downarrow\downarrow\uparrow\rangle + |\downarrow\uparrow\downarrow\rangle + |\uparrow\downarrow\downarrow\rangle)$ . This rewriting can be carried out on any lattice of triangles; if a bond is used by multiple triangles this constrains the coupling constant between these bonds.

The  $XXZ0$  Hamiltonian is thus a sum of positive semi-definite non-commuting projectors. Any wavefunction that simultaneously zeroes out each projector consistently is guaranteed to be a ground state. Such "frustration-free" Hamiltonians include Majumdar-Ghosh [28] (generalized by Klein [29]) and Affleck-Kennedy-Lieb-Tasaki [30–33] Hamiltonians. Zeroing out a projector requires that only components exactly

orthogonal to states  $|+\rangle$  and  $|-\rangle$  enter the full many body wavefunction; this is indeed achieved by the product state  $|\psi\rangle \equiv \prod_{\text{valid}} \otimes |\gamma_s\rangle$ . We also note that such "three-coloring states" have a long history and have been explored in several contexts [24, 34–40].

The product state  $|\psi\rangle$  does not conserve total  $S_z$  but the  $XXZ$  Hamiltonian *does conserve* it. Therefore, projecting each three-coloring solution to each  $S_z$  sector is also a ground state leading to Eq. (3). Note that three-colorings which differ simply by relabeling colors are identical up to a global phase (see Supplement).

*Macroscopic Degeneracy and additional ground states*— While there are only two ways of three-coloring the triangular lattice, there are an exponential number of ways of doing so on the kagome (scaling as  $1.208^N$  [41]) and hyper-kagome lattices. The precise number of ground states varies from sector to sector because of the loss of linear independence of the unprojected solutions under projection. For typical  $S_z$  of interest, particularly  $S_z = 0$ , there are still an exponential number of linearly independent solutions. This counting is made precise by forming the overlap matrix  $S_{C,C'} \equiv \langle C|C'\rangle$  and evaluating its rank  $\equiv R(S)$  numerically; our results have been shown in Table I and the Supplement. The case of one down spin in a sea of up spins which maps to the non-interacting problem with a flat-band with a quadratic band touching [42] is also correctly captured.

On several representative clusters with open boundary conditions (but always with completed triangles), we never find solutions outside the coloring manifold which suggests (but does not prove) the possibility that coloring solutions describe all degeneracies on open lattices. However, for kagome on tori we find, for low fillings, degenerate solutions not spanned by colorings.

*Connection to the wider Kagome phase diagram*— We now show how the  $XXZ0$  point is embedded in the larger kagome phase diagram. We focus on  $S_z = 0$  and the fully symmetric sector of  $K = (0, 0)$  sector (see Supplement), and study an extended Hamiltonian involving nearest neighbor (nn) and next-nearest neighbor (nnn) terms,

$$H[J_z, J_2] = H_{XXZ}^{\text{nn}}[J_z] + J_2 H_{XXZ}^{\text{nnn}}[J_z] \quad (5)$$

where  $H_{XXZ}^{\text{nnn}}[J_z] = \left( \sum_{\langle\langle i,j \rangle\rangle} S_i^x S_j^x + S_i^y S_j^y + J_z S_i^z S_j^z \right)$ ;  $\langle\langle i,j \rangle\rangle$  referring to nnn pairs. We use a combination of analytical arguments and ED on the 36d cluster [43, 44] on a grid of points in the  $(J_z, J_2)$  space. As Fig. 3 shows, we find five phases near  $XXZ0$ : a ferromagnetic phase, a  $q = 0$  phase, a  $\sqrt{3} \times \sqrt{3}$  phase and (potentially) two spin-liquids. We give numerical evidence that all these phases, other than the ferromagnet, connect from near (or touching)  $XXZ0$  to the Heisenberg point.

At  $J_z = -1/2$  and  $J_2 > 0$ , (notated AF-line) all triangles in the Hamiltonian are of the  $XXZ0$  form and remain consistently three-colorable. Three-coloring both nn and nnn triangles constrains the allowed colorings leaving only two colorings in the well known  $q = 0$  pattern. This phase sur-

Lattice	Method	$n_b = 1$	$n_b = 2$	$n_b = 3$	$n_b = 4$	$n_b = 5$	$n_b = 6$	$n_b = \lfloor N/2 \rfloor$	# 3-colorings
sawtooth obc	ED	6	16	26	31	32	32	32	32
5 triangles	$R(S)$	6	16	26	31	32	32	32	
$3 \times 3$ kagome obc (33 sites)	ED	15	102	414	1117				3808
	$R(S)$	15	102	414	1117	2136	3078	3808	
$3 \times 3$ kagome pbc	ED	10	38	60	41	40	40	40	40
	$R(S)$	10	34	40	40	40	40	40	
$4 \times 3$ kagome pbc	ED	13	68	169	172	137	136		136
	$R(S)$	13	68	134	136	136	136	136	

Table I. Number of ground states in different  $S_z$  sectors (mapped to hard-core boson number  $n_b$ ) on several lattices (of size  $N$ ) with triangular motifs at  $J_z = -1/2$ ,  $J_2 = 0$ .  $R(S)$  is the rank of the overlap matrix indicating the number of linearly independent 3-coloring modes and ED refers to the exact number of ground states. The kagome cluster with open boundary conditions (obc) has completed triangles, resembling the periodic counterpart (pbc) in appearance.

vives for  $J_z > -1/2$ , at small  $J_2$ , and is primarily identified by peaks at the  $M$  point (Fig. S2 of the Supplement) in the spin-structure factor  $S(\vec{q}) \equiv \frac{1}{N} \sum_{i,j} \langle S_i \cdot S_j \rangle e^{i\vec{q} \cdot (\vec{r}_i - \vec{r}_j)}$  where  $\vec{r}_i$  refers to the real space coordinates of the  $i^{\text{th}}$  lattice site,  $N$  is the total number of sites and  $\langle S_i \cdot S_j \rangle$  is the spin-spin correlation function. On the other hand, it can be rigorously shown the minimum energy state upon perturbing the AF-line to  $J_z < -1/2$  is the fully polarized ferromagnetic state.

At  $J_z = -1/2$  and  $J_2 < 0$ , we find evidence for the  $\sqrt{3} \times \sqrt{3}$  phase. While we can not solve for the exact ground state, the state which colors nnn triangles the same color (i.e. the  $\sqrt{3} \times \sqrt{3}$  phase) minimizes the nnn energy within the three-coloring manifold. We numerically verify this phase by looking at  $S(K)$ , finding it survives for  $J_z$  near and on both sides of  $-1/2$ .

By tracing paths through parameter space with large values of  $S(\vec{q})$  at the  $K$  and  $M$  points, we find that both the  $q = 0$  phase and  $\sqrt{3} \times \sqrt{3}$  phases near the  $XXZ0$  point extend to the Heisenberg point at non-zero  $J_2$ . To locate the boundaries of these phases, we perform sweeps through  $J_2$  at fixed  $J_z$  and identify dips in the wavefunction fidelity defined to be

$$f(J_z, J_2) \equiv \left| \langle \psi(J_z, J_2 - \Delta J_2/2) | \psi(J_z, J_2 + \Delta J_2/2) \rangle \right| \quad (6)$$

where  $\psi(J_z, J_2)$  is the ground state wavefunction,  $\Delta J_2$  is the step size in the  $J_2$  direction. For both magnetically ordered phases, the location of these dips form lines emanating from (or close to) the  $XXZ0$  point that extrapolate to the Heisenberg point ( $J_z = 1$ ) to values  $J_2 \approx 0.16$  for  $q = 0$  and  $J_2 \approx -0.06$  for  $\sqrt{3} \times \sqrt{3}$ . These values are within the bounds previously found by a DMRG study [45], but disagree with a variational study by Ref. [46] which finds instead a valence bond crystal. In the intermediate phase(s), we see a decrease in the magnitude of the structure factor peaks consistent with a change in phase to a spin-liquid.

Near  $XXZ0$  we do not detect fidelity dips and see larger structure factors that extend much closer to the line  $J_2 = 0$ . This leaves two plausible scenarios: (1) the spin-liquid(s) terminate at  $J_z > -1/2$  for all  $J_2$  or (2) the phase boundaries

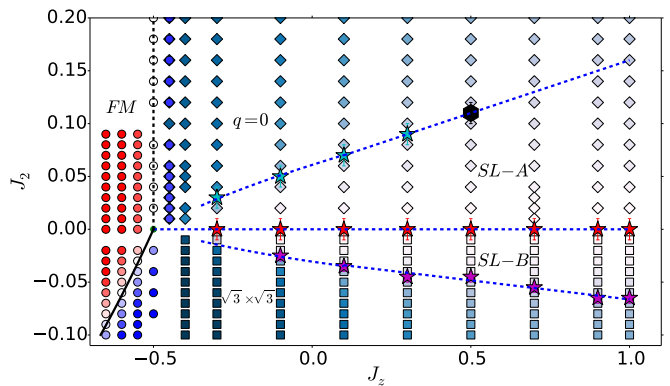


Figure 3. (Color online): The phase diagram in the  $J_z - J_2$  plane on the 36d lattice showing five phases - the ferromagnet (FM), the magnetically ordered phases ( $q = 0$  and  $\sqrt{3} \times \sqrt{3}$ ), and the spin liquids (SL-A and SL-B). Circles correspond to the energy difference  $E(S_z = 0)_{N=36} - E_{TDL}(S_z = N/2)$  between the  $S_z = 0$  sector and fully polarized state ranging from deep blue (negative) to deep red (positive). The diamonds are colored based on the structure factor at the  $M$  point ( $S(M)$ ) and squares are colored based on the structure factor at the  $K$  point ( $S(K)$ ). The darkest color corresponds to the largest structure factor on the graph. Star symbols correspond to location of fidelity dips and the error-bars indicate the uncertainty in the location of the phase boundaries (when scanned in the  $J_2$  direction) and correspond to the grid-spacing used for the computation of the fidelity. The black hexagon (at  $J_z \approx 0.5$ ,  $J_2 \approx 0.10$ ) is a kink in the second derivative of the fidelity; beyond the corresponding  $J_z$  the fidelity dip is not noticeable and the phase boundary is just an extrapolation. Phase boundaries are marked with dotted lines, which are guides to the eye. The solid line is where the semiclassical energy difference between the FM and the unprojected  $\sqrt{3} \times \sqrt{3}$  state goes to zero.

extend to  $XXZ0$  but finite size-effects near it become large making it difficult to resolve the transition.

We find an additional fidelity dip at  $J_2 \approx 0$  and  $J_z > -1/2$  in the region where other studies [45] identify a single spin-liquid phase. This interesting finding indicates the existence of an additional transition in this region. Our analysis in this work is largely ambivalent about the nature of these two phases but earlier evidence for a spin-liquid phase at  $J_z = 1$

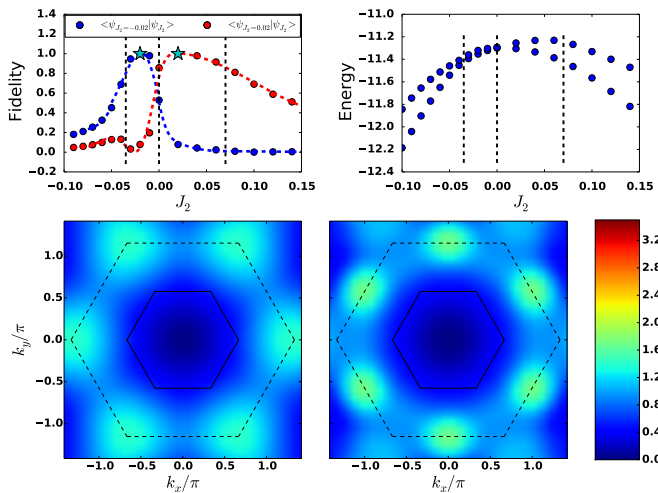


Figure 4. (Color online) All data is at  $J_z = 0.1$  for the 36d lattice. Top Left: Overlap of the ground state at  $J_2$  with respect to reference ground state wavefunctions at  $J_2 = -0.02$  (blue) and  $J_2 = 0.02$  (red). Dashed lines represent transitions as measured by fidelity. Top Right: Energy of the two lowest states in the symmetric representation of the  $K = (0, 0)$  sector. There are additional state(s) between these two states in other quantum-number sectors. Bottom: The static spin structure factor  $S(\vec{q})$  of the ground state for  $J_2 = -0.02$  (left) and  $J_2 = 0.02$  (right). The solid and the dotted lines show the first and the extended Brillouin zones respectively. The high symmetry points of the latter correspond to  $K$  (corners of the hexagon) and  $M$  (midpoints of edges) points. On going from  $J_2 < 0$  to  $J_2 > 0$ , the intensity is transferred from  $K$  to  $M$  points.

and both  $J_2 > 0, J_2 < 0$  [14, 45] suggests a possible transition between two spin-liquids. Interestingly, a recent IPEPS study [47] found nearly degenerate variational degenerate energies for the  $Q_1 = Q_2$  and  $Q_1 = -Q_2$  [38]  $Z_2$ -spin liquids which they interpret as evidence for a parent  $U(1)$  DSL; given our results, another reasonable interpretation is that there is a transition between these two states.

To further understand the nature of the fidelity dips, we consider the ground state and excited state in the same quantum number sector as a function of  $J_2$  at  $J_z = 0.1$  (Fig. 4, top right); the true first excited-state is in another sector. We see a (formally avoided) "level-crossing" indicated by a shrinking gap between these states around  $J_2 \approx 0$ . This crossing causes the fidelity dip and leads to the overlap of the wavefunction on both sides of  $J_2 \approx 0$  being small with respect to a reference point on the other side (see Fig. 4, top left). In addition, the structure factors of the two ground states at positive and negative  $J_2$ , despite not having large peaks, are qualitatively distinct (see Fig. 4, bottom).

*Conclusion*— In summary, we have (1) shown that  $H_{XXZ0}$  is macroscopically quantum degenerate on the kagome and hyperkagome lattices, (2) shown that all projected three-coloring states are exact ground states of  $H_{XXZ0}$  on any three-colorable lattice of triangular motifs explaining this macroscopic degeneracy, (3) shown that multiple phases in the  $J_2 - J_z$  phase diagram, including the spin-liquid(s) at the KAHF, are proximate to the  $XXZ0$  point, and (4) given evidence for a transition

between two phases at  $J_2 = 0$  for  $-0.5 < J_z < 1$ . Our findings suggest that the  $XXZ0$  point controls the physics of the Heisenberg and  $XY$  points [15, 48] on the kagome and the existence of a transition near the KAHF might help resolve conflicting numerical evidence for gapless and gapped states respectively. While our focus here has been on the uniform kagome lattice, the exponential degeneracy also applies in the case where the coupling constant in each triangle is disordered (or staggered) as well as to finite clusters of triangles such as the icosidodecahedron; in fact, the latter explains the nearly degenerate manifold on this cluster in the  $XY$  regime [49].

The central coloring ideas extend to other frustrated lattices with four (or higher) site motifs [50–52]. For example, define a Hamiltonian which annihilates four-coloring states made of one  $a \equiv |\uparrow\rangle + |\downarrow\rangle$ ,  $b \equiv |\uparrow\rangle + i|\downarrow\rangle$ ,  $c \equiv |\uparrow\rangle - |\downarrow\rangle$  and  $d \equiv |\uparrow\rangle - i|\downarrow\rangle$  on each square of a square lattice or tetrahedron of the pyrochlore lattice. Up to a constant, this is  $H = 2H_{XXZ}[-1/4] + \sum_{i<j,k<l,\text{diff}} S_i^+ S_j^+ S_k^- S_l^- - 2 S_1^z S_2^z S_3^z S_4^z$  where "diff" indicates  $i, j, k, l$  are distinct (see Supplement for the derivation that used the DiracQ package [53]). Notice that on the square this forces the  $nnn J_2$  coupling to be half the  $nn J_1$  coupling; interestingly  $J_2/J_1 = 1/2$  has been proposed to be a SL state on the square for Heisenberg and  $XY$  models [54]. We believe that the macroscopic degeneracy of this Hamiltonian on the square and pyrochlore lattices will be a source of multiple phases on these lattices [55, 56].

Finally, we note that three-coloring states can be used to construct accurate many-body wavefunctions [12, 57–59]. Typically Jastrow factors have been introduced only on top of a single coloring; our present investigation suggests that a linear combination of colorings may provide accurate results in the vicinity of the  $XXZ0$  point.

*Acknowledgement*— We thank V. Elser, S. Shastry, O. Tchernyshyov, V. Chua, L.D.C Jaubert, S. Sachdev, R. Flint, P. Nikolic, Y. Wan and O. Benton for discussions and H. Wang for collaboration on related work. We also thank T. Momoi for bringing to our attention Ref. [25] after this work was posted. HJC, DK and BKC were supported by SciDAC grant DE-FG02-12ER46875 and KK and EF by NSF grant numbers DMR 1408713 and 1725401. HJC also acknowledges funding from the U.S. Department of Energy, Office of Basic Energy Sciences, Division of Materials Sciences and Engineering under Award DE-FG02-08ER46544 for his work at the Institute for Quantum Matter (IQM). This research is part of the Blue Waters sustained petascale computing project, which is supported by the National Science Foundation (award numbers OCI-0725070 and ACI-1238993) and the State of Illinois.

- 
- [1] P. Anderson, *Materials Research Bulletin* **8**, 153 (1973).
  - [2] J. S. Helton, K. Matan, M. P. Shores, E. A. Nytko, B. M. Bartlett, Y. Yoshida, Y. Takano, A. Suslov, Y. Qiu, J.-H. Chung, D. G. Nocera, and Y. S. Lee, *Phys. Rev. Lett.* **98**, 107204 (2007).
  - [3] Y. Okamoto, M. Nohara, H. Aruga-Katori, and H. Takagi,

- Phys. Rev. Lett. **99**, 137207 (2007).
- [4] C. Zeng and V. Elser, *Phys. Rev. B* **42**, 8436 (1990).
- [5] R. R. P. Singh and D. A. Huse, *Phys. Rev. B* **76**, 180407 (2007).
- [6] Y. Ran, M. Hermele, P. A. Lee, and X.-G. Wen, *Phys. Rev. Lett.* **98**, 117205 (2007).
- [7] S. Yan, D. A. Huse, and S. R. White, *Science* **332**, 1173 (2011).
- [8] S. Depenbrock, I. P. McCulloch, and U. Schollwöck, *Phys. Rev. Lett.* **109**, 067201 (2012).
- [9] Y. Iqbal, F. Becca, S. Sorella, and D. Poilblanc, *Phys. Rev. B* **87**, 060405 (2013).
- [10] H.-C. Jiang, Z. Wang, and L. Balents, *Nat. Phys.* **8**, 902 (2012).
- [11] B. K. Clark, J. M. Kinder, E. Neuscamman, G. K.-L. Chan, and M. J. Lawler, *Phys. Rev. Lett.* **111**, 187205 (2013).
- [12] T. Tay and O. I. Motrunich, *Phys. Rev. B* **84**, 020404 (2011).
- [13] Y.-C. He, M. P. Zaletel, M. Oshikawa, and F. Pollmann, *Phys. Rev. X* **7**, 031020 (2017).
- [14] H. J. Liao, Z. Y. Xie, J. Chen, Z. Y. Liu, H. D. Xie, R. Z. Huang, B. Normand, and T. Xiang, *Phys. Rev. Lett.* **118**, 137202 (2017).
- [15] Y.-C. He and Y. Chen, *Phys. Rev. Lett.* **114**, 037201 (2015).
- [16] H. J. Changlani and A. M. Läuchli, *Phys. Rev. B* **91**, 100407 (2015).
- [17] N. Y. Yao, M. P. Zaletel, D. M. Stamper-Kurn, and A. Vishwanath, ArXiv e-prints (2015), [arXiv:1510.06403](https://arxiv.org/abs/1510.06403) [cond-mat.str-el].
- [18] D. Yamamoto, G. Marmorini, and I. Danshita, *Phys. Rev. Lett.* **112**, 127203 (2014).
- [19] D. Sellmann, X.-F. Zhang, and S. Eggert, *Phys. Rev. B* **91**, 081104 (2015).
- [20] A. L. Chernyshev and M. E. Zhitomirsky, *Phys. Rev. Lett.* **113**, 237202 (2014).
- [21] O. Götze and J. Richter, *Phys. Rev. B* **91**, 104402 (2015).
- [22] K. Kumar, K. Sun, and E. Fradkin, *Phys. Rev. B* **90**, 174409 (2014).
- [23] K. Kumar, H. J. Changlani, B. K. Clark, and E. Fradkin, *Phys. Rev. B* **94**, 134410 (2016).
- [24] K. Essafi, O. Benton, and L. D. C. Jaubert, *Nat. Commun.* **7**, 10297 (2016).
- [25] T. Momoi and M. Suzuki, *Journal of the Physical Society of Japan* **61**, 3732 (1992).
- [26] C. D. Batista, *Phys. Rev. B* **80**, 180406 (2009).
- [27] B. S. Shastry and B. Sutherland, *Physica B+C* **108**, 1069 (1981).
- [28] C. K. Majumdar and D. K. Ghosh, *Journal of Mathematical Physics* **10**, 1388 (1969).
- [29] D. J. Klein, *Journal of Physics A: Mathematical and General* **15**, 661 (1982).
- [30] I. Affleck, T. Kennedy, E. H. Lieb, and H. Tasaki, *Phys. Rev. Lett.* **59**, 799 (1987).
- [31] X.-G. Wen, *Phys. Rev. Lett.* **90**, 016803 (2003).
- [32] A. Kitaev, *Annals of Physics* **303**, 2 (2003).
- [33] H. Wang, H. J. Changlani, Y. Wan, and O. Tchernyshyov, *Phys. Rev. B* **95**, 144425 (2017).
- [34] A. B. Harris, C. Kallin, and A. J. Berlinsky, *Phys. Rev. B* **45**, 2899 (1992).
- [35] C. L. Henley, *Phys. Rev. B* **80**, 180401 (2009).
- [36] D. A. Huse and A. D. Rutenberg, *Phys. Rev. B* **45**, 7536 (1992).
- [37] J. T. Chalker, P. C. W. Holdsworth, and E. F. Shender, *Phys. Rev. Lett.* **68**, 855 (1992).
- [38] S. Sachdev, *Phys. Rev. B* **45**, 12377 (1992).
- [39] O. Cépas and A. Ralko, *Phys. Rev. B* **84**, 020413 (2011).
- [40] C. Castelnovo, C. Chamon, C. Mudry, and P. Pujol, *Phys. Rev. B* **72**, 104405 (2005).
- [41] R. J. Baxter, *Journal of Mathematical Physics* **11**, 784 (1970).
- [42] D. L. Bergman, C. Wu, and L. Balents, *Phys. Rev. B* **78**, 125104 (2008).
- [43] P. W. Leung and V. Elser, *Phys. Rev. B* **47**, 5459 (1993).
- [44] A. M. Läuchli, J. Sudan, and E. S. Sørensen, *Phys. Rev. B* **83**, 212401 (2011).
- [45] F. Kolley, S. Depenbrock, I. P. McCulloch, U. Schollwöck, and V. Alba, *Phys. Rev. B* **91**, 104418 (2015).
- [46] Y. Iqbal, F. Becca, and D. Poilblanc, *New Journal of Physics* **14**, 115031 (2012).
- [47] S. Jiang, P. Kim, J. H. Han, and Y. Ran, arXiv preprint [arXiv:1610.02024](https://arxiv.org/abs/1610.02024) (2016).
- [48] A. M. Läuchli and R. Moessner, ArXiv e-prints (2015), [arXiv:1504.04380](https://arxiv.org/abs/1504.04380) [cond-mat.quant-gas].
- [49] I. Rousochatzakis, A. M. Läuchli, and F. Mila, *Phys. Rev. B* **77**, 094420 (2008).
- [50] J. Kondev and C. L. Henley, *Nuclear Physics B* **464**, 540 (1996).
- [51] V. Khemani, R. Moessner, S. A. Parameswaran, and S. L. Sondhi, *Phys. Rev. B* **86**, 054411 (2012).
- [52] Y. Wan and M. J. P. Gingras, *Phys. Rev. B* **94**, 174417 (2016).
- [53] J. G. Wright and B. S. Shastry, ArXiv e-prints (2013), [arXiv:1301.4494](https://arxiv.org/abs/1301.4494) [cond-mat.str-el].
- [54] Y.-H. Chan and L.-M. Duan, *New Journal of Physics* **14**, 113039 (2012).
- [55] B. Normand and Z. Nussinov, *Phys. Rev. Lett.* **112**, 207202 (2014).
- [56] M. Hermele, M. P. A. Fisher, and L. Balents, *Phys. Rev. B* **69**, 064404 (2004).
- [57] D. A. Huse and V. Elser, *Phys. Rev. Lett.* **60**, 2531 (1988).
- [58] H. J. Changlani, J. M. Kinder, C. J. Umrigar, and G. K.-L. Chan, *Phys. Rev. B* **80**, 245116 (2009).
- [59] E. Neuscamman, H. Changlani, J. Kinder, and G. K.-L. Chan, *Phys. Rev. B* **84**, 205132 (2011).